Atmos. Meas. Tech. Discuss., 5, 5205–5243, 2012
www.atmos-meas-tech-discuss.net/5/5205/2012/
doi:10.5194/amtd-5-5205-2012

Atmospheric Measurement Techniques Discussions

Accuracy assessment of Aqua-MODIS aerosol optical depth over coastal regions: importance of quality flag and sea surface wind speed

J. C. Anderson[1], J. Wang[1], J. Zeng[1], M. Petrenko[2,3], G. G. Leptoukh[2,†], and C. Ichoku[2]

[1]Department of Earth and Atmospheric Science, University of Nebraska-Lincoln, Lincoln, NE, USA
[2]NASA Goddard Space Flight Center, Greenbelt, MD, USA
[3]Earth System Science Interdisciplinary Center, University of Maryland, College Park, MD, USA
[†]deceased

Received: 8 July 2012 – Accepted: 11 July 2012 – Published: 26 July 2012

Correspondence to: J. Wang (jwang7@unl.edu)

Published by Copernicus Publications on behalf of the European Geosciences Union.

Abstract

Coastal regions around the globe are a major source for anthropogenic aerosols in the atmosphere, but the underlying surface characteristics are not favorable for the Moderate Resolution Imaging Spectroradiometer (MODIS) algorithms designed for retrieval of aerosols over dark land or open-ocean surfaces. Using data collected from 62 coastal stations worldwide from the Aerosol Robotic Network (AERONET) from ~2002–2010, accuracy assessments are made for coastal aerosol optical depth (AOD) retrieved from MODIS aboard Aqua satellite. It is found that coastal AODs (at 550 nm) characterized respectively by the MODIS Dark Land (hereafter Land) surface algorithm, the Open-Ocean (hereafter Ocean) algorithm, and AERONET all exhibit a log-normal distribution. After filtering by quality flags, the MODIS AODs respectively retrieved from the Land and Ocean algorithms are highly correlated with AERONET (with $R^2 \approx 0.8$), but only the Land algorithm AODs fall within the expected error envelope greater than 66 % of the time. Furthermore, the MODIS AODs from the Land algorithm, Ocean algorithm, and combined Land_and_Ocean product show statistically significant discrepancies from their respective counterparts from AERONET in terms of mean, probability density function, and cumulative density function, which suggest a need for future improvement in retrieval algorithms. Without filtering with quality flag, the MODIS Land_and_Ocean AOD dataset can be degraded by 30–50 % in terms of mean bias. Overall, the MODIS Ocean algorithm overestimates the AERONET coastal AOD by 0.021 for AOD < 0.25 and underestimates it by 0.029 for AOD > 0.25. This dichotomy is shown to be related to the ocean surface wind speed and cloud contamination effects on the satellite aerosol retrieval. The Modern Era Retrospective-Analysis for Research and Applications (MERRA) reveals that wind speeds over the global coastal region (with a mean and median value of 2.94 $m\,s^{-1}$ and 2.66 $m\,s^{-1}$, respectively) are often slower than 6 $m\,s^{-1}$ assumed in the MODIS Ocean algorithm. As a result of high correlation ($R^2 > 0.98$) between the bias in binned MODIS AOD and the corresponding binned wind speed over the coastal sea surface, an empirical scheme for correcting

AMTD
5, 5205–5243, 2012

the bias of AOD retrieved from the MODIS Ocean algorithm is formulated and is shown to be effective over the majority of the coastal AERONET stations, and hence can be used in future analysis of AOD trend and MODIS AOD data assimilation.

1 Introduction

Aerosols play an important role in the Earth's energy balance and hydrological cycle (Charlson et al., 1992) through scattering and absorbing radiation (direct affect), as well as influencing cloud radiative effects through the modification of their microphysical properties in the atmosphere (indirect affect). These airborne particles also reduce visibility and affect human health (Samet et al., 2000). The Intergovernmental Panel on Climate Change (IPCC) in their fourth assessment reports that the direct aerosol radiative forcing is best estimated as $-0.5\,\mathrm{W\,m^{-2}}$, rendering a cooling powerful enough to offset the warming from CO_2 by almost one-third (Myhre, 2009). However, the uncertainties associated with this best estimate are close to 80 %, i.e., the range of aerosol radiative forcing is from -0.1 to $-0.9\,\mathrm{W\,m^{-2}}$ (IPCC, 2007). Further reduction of such large uncertainties, especially through observation-based characterization of aerosol properties on a global scale, is needed for improved prediction of climate change (IPCC, 2007). Since the IPCC report in 2007, various studies have evaluated the trends of Aerosol Optical Depth (AOD), the first-order indication of columnar aerosol mass and aerosol forcing, using the data retrieved from different satellite sensors, including the Moderate Resolution Imaging Spectroradiometer (MODIS), Advanced Very High Resolution Radiometer (AVHRR), and Multi-Angle Imaging Spectroradiometer (MISR). However, these past evaluations only studied the trend of aerosols over the open-ocean and show inconsistent results (Mishchenko and Geogdzhayev, 2007; Remer et al., 2008; Zhang and Reid, 2006; Zhao et al., 2011), with both positive and negative trends estimated in global averages reported by Mishchenko et al. (2007) and Zhang and Reid (2010), respectively.

AMTD
5, 5205–5243, 2012

In the context of trend analysis of satellite-based AOD, this study focuses on the evaluation and refinement of the accuracy of AOD retrieved from MODIS over the coastal regions. Since its inception, the MODIS level 2 aerosol product, due to its daily and nearly global coverage, has been used widely in research literature for studying aerosol processes ranging from source, transport, and deposition to impacts on air quality and climate (Bhaskaran et al., 2011; Bréon et al., 2011; Chatterjee et al., 2010; Kahn et al., 2011, 2007, 2005; Levy et al., 2007a, 2010; Mi et al., 2007; Remer et al., 2005; Smirnov et al., 2011; and others). World-wide comparisons of MODIS AOD with those measured from AERONET show that the MODIS AOD product overall has an accuracy of $\pm(0.05 + 0.15 \cdot \mathrm{AOD}_{\mathrm{actual}})$ over the land and $\pm(0.03 + 0.05 \cdot \mathrm{AOD}_{\mathrm{actual}})$ over the ocean (Levy et al., 2007a, 2010; Remer et al., 2005; Kahn et al., 2011, 2007, 2005). Such uncertainty brackets the value of the AOD trend, at 550 nm, of −0.03 from 1991 to 2005 reported by Mishchenko et al. (2007) and of 0.003 per decade found by Zhang and Reid, (2010). Furthermore, the MODIS AOD uncertainty at regional scales on either land or ocean can be much greater than on a global scale (Levy et al., 2005), because the accuracy of aerosol retrievals is subject to the change of boundary conditions and surface types (Levy et al., 2007b). In this regard, the MODIS AOD products over the coastal regions deserve special attention because: (a) they are a simple union of the retrievals from algorithms that are designed for either over land only or over open-ocean only, and (as discussed below) neither algorithm has a dedicated scheme to characterize the surface reflectance at the coast that are often influenced by a sand-water mixture and water-leaving radiance contributed by the underlying sea shore and suspended matter in shallow ocean water; (b) over half the world's population resides in the coastal region (Tibbetts, 2002), which makes assessment of AOD over the coastal region critical for understanding the global trend of Aerosol Optical Depth (AOD), especially anthropogenic AOD, and may have important implications for future air quality studies.

Both MODIS aerosol retrieval algorithms over dark surfaces, i.e., the Open-Ocean (hereafter Ocean) algorithm and the Dark Land (hereafter Land) algorithm, use the

AMTD
5, 5205–5243, 2012

cloud-free Top Of the Atmosphere (TOA) reflectances that are measured at resolutions ranging from 250 m in the shortwave visible wavelengths to 500 m in the near-infrared and are then aggregated to boxes of 20 by 20 (500 m resolution) pixels or equivalent to 10 by 10 km resolution at nadir for aerosol retrieval (Remer et al., 2005). The Ocean algorithm is used for retrieval if all pixels within the 20 × 20-pixel box are water; otherwise, the Land algorithms are used. Determining if a pixel is over land or over water is based upon the MOD35 1-km data that contains information about surface type (Remer et al., 2005). To date, a simple union of the AODs retrieved from the Land and Ocean algorithms make up the MODIS, level 2, "Land_and_Ocean" AOD product that is popularly used in the research community.

However, such a simple union of separate retrievals from the Land and Ocean algorithms renders several difficulties for the evaluation of MODIS AOD retrievals over the coastal regions. First, the algorithm used for AOD retrieval in the same location can vary with the time or with the MODIS ground track. This can be understood because the pixel resolution at the ground is a function of satellite viewing zenith angle. With a repeat cycle of 16 days, a box of MODIS 20 by 20 pixels can be exactly equal to 10 by 10 km^2 when viewed by MODIS at nadir, but can also be equivalent to 20 by 48 km^2 area when viewed by MODIS at the high viewing zenith angle. Even if the AOD for 20 by 20 pixels over a coastal ocean region will be retrieved by the Ocean algorithm in the nadir situation, in the latter case, the 20 by 20 pixels on which the MODIS algorithm operates can possibly contain one or more land pixel(s), and therefore the Land algorithm may be applied for the same coastal region. Secondly, a simple merge of the Land and Ocean retrievals, as now implemented in MODIS collection-5.1 algorithm, renders a loss of retrieval quality information that is associated with Land and Ocean retrievals, respectively.

Besides the aforementioned two issues associated with the simple data merge of MODIS AOD over the coast, this study will also look into the assumptions made by the MODIS Look Up Tables (LUTs) corresponding to the ocean surface characteristics. Inherent in the MODIS LUT are assumptions about the ocean surface (Kleidman

AMTD
5, 5205–5243, 2012

et al., 2012). Three ocean surface properties are particularly important in the Ocean algorithm: water-leaving radiance, rough ocean surface causing changes in sun glint patterns, and white caps (Kleidman et al., 2012). The spectral water-leaving radiances are determined by suspended material in the surface layer, and can be influenced by shallow ocean floor reflectance. Therefore, these values can vary significantly from open-ocean to coastal ocean. However, such variation is not considered in the current MODIS aerosol algorithm that assumes 0.0 water leaving radiances for all but the 550 nm channel where a value of 0.005 is assumed (Remer et al., 2005).

The Ocean algorithm uses a Cox and Munk (1954) rough ocean surface model to provide the sun glint pattern. The algorithm masks all geometry within 40 degrees of specular reflection. Both the glint patterns and the white caps are determined by surface wind speed. The MODIS aerosol algorithm assumes a constant $6\,m\,s^{-1}$ wind speed for all retrievals. A Koepke (1984) model is used to estimate the white cap reflectance contribution. Thus, the assumed wind speed of $6\,m\,s^{-1}$ in the algorithm needs to be evaluated. Kleidman et al. (2012) demonstrate the dependence of the MODIS aerosol accuracy over the open-ocean on surface wind speed, and show that significant error can arise when wind speeds are faster or slower than $6\,m\,s^{-1}$. This can be understood because the ocean surface has greater reflectance with higher wind speeds and lower reflectance at slower wind speeds. The change in the ocean surface reflectance due to wind speed is not accounted for in the Ocean algorithm leading to an overestimation of AOD for wind speeds greater than $6\,m\,s^{-1}$ and an underestimation for wind speeds less than $6\,m\,s^{-1}$. Previous evaluations of the Ocean algorithm that have studied the effect of wind speed (Kleidman et al., 2012; Shi et al., 2011; Zhang and Reid, 2006) and cloud contamination (Zhang and Reid, 2006, 2010) on retrievals of aerosols, however, are restricted to the open-ocean, and hence, the evaluation of the effect of cloud contamination and assumed sea surface wind speed on aerosol retrievals over coastal oceans needs further assessment.

This paper is designed to address three issues as discussed in the previous paragraphs, i.e., the overall accuracy of MODIS AOD over the coast, and how they are

AMTD
5, 5205–5243, 2012

related to the effects of the quality flag and sea surface wind speed. To avoid the issues related to MODIS/Terra calibration (Remer et al., 2005), we here only evaluate the accuracy of MODIS/Aqua AOD. We introduce the data used in this study in Sect. 2, evaluate the performance of the MODIS Ocean and Land aerosol algorithms over coastal regions in Sect. 3, develop a quality control method for the MODIS Land_and_Ocean data set in Sect. 4, present the analysis of MODIS AOD bias due to cloud contamination and the assumption of sea surface wind speed in Sect. 5, and finally summarize the findings in Sect. 6.

2 Data description, collocation, and classification for AERONET coastal sites

An overview of the data products used for this research is provided in the first part of this section, including the MODIS aerosol algorithms, AERONET aerosol measurements and surface wind speed data set. This is followed by the discussion of the processes used for collocating MODIS and AERONET AOD.

2.1 MODIS and AERONET AOD products

MODIS AOD is reported at 7 wavelengths (470 nm, 550 nm, 660 nm, 870 nm, 1200 nm, 1600 nm, 2100 nm) for the Ocean algorithm and four wavelengths (470 nm, 550 nm, 660 nm, 2100 nm) for the Land algorithm. The 550 nm wavelength is used for comparison with AERONET because it is consistent with the primary wavelength used by many climate and chemistry transport models (Kinne et al., 2003) as well as previous MODIS validation studies (Levy et al., 2007a, 2010; Remer et al., 2005). Note that vegetatedsurfaces are not "dark" in the 550 nm wavelength, and therefore, the AOD at this wavelengthover land is derived from the retrieved AODs at multiple MODIS channels (Levy et al., 2010).

The MODIS aerosol algorithms operate through the use of LUTs in order to estimate AOD (Levy et al., 2010). The LUTs store the top-of-atmosphere (TOA) spectral

AMTD
5, 5205–5243, 2012

reflectance from pre-computed radiative transfer with the assumptions that only a small set of aerosol types, loadings, and geometries can represent the global range of aerosol conditions (Levy et al., 2010; Kaufman et al., 1997). The LUTs represent spectrally consistent atmospheric properties computed for different aerosol types that are classified according to AERONET characterization and vary with geographical location and season (Levy et al., 2010). The spectral surface reflectance contribution is constrained by the 2.1/0.67 μm reflectance ratio, and further description of the parameterization is described by Levy et al. (2007b). Thus, with the surface contribution "known", the MODIS observed TOA reflectance at the 470 nm and 660 nm wavelengths can be compared to the LUT to determine the best-fit AOD. The best fit represents the solution that provides the smallest fitting error when matching the LUT spectral reflectances to MODIS observation (Levy et al., 2010).

Only the most recent MODIS collection (now 5.1), quality assured, level 2 data are used. MODIS uses quality flags to represent the accuracy of AOD retrievals. The quality flags range from 3 (high confidence) to 0 (low or no confidence) (Levy et al., 2010). It has been shown in previous research that the quality flags associated with MODIS retrievals play a significant role in MODIS AOD error approximation (Levy et al., 2010; Remer et al., 2005). The Expected Error (EE) envelope for the MODIS aerosol algorithms are represented by $EE = \pm(0.05 + 0.15 \cdot AOD_{actual})$ for the land algorithm, and $EE = \pm(0.03 + 0.05 \cdot AOD_{actual})$ for the ocean algorithm (Remer et al., 2005), here AOD_{actual} is equal to the AOD retrieved from AEROENT. The retrievals that fall within the EE bound (greater than 66 % of the time), on a global average, are represented by the quality flag 3 for the land algorithm, and the flags 1, 2, and 3 for the ocean algorithm (Remer et al., 2005; Levy et al., 2010).

AERONET derives AOD from direct sun photometer measurements in some or all of the following seven different spectral bands centered at 340 nm, 380 nm, 440 nm, 500 nm, 670 nm, 940 nm, and 1020 nm (Holben et al., 1998). AERONET measures the extinction of direct beam solar radiation, and applies the Beer-Lambert-Bouguer law to determine AOD (Holben et al., 1998) with uncertainties on the order of 0.01–0.02 (Eck

AMTD
5, 5205–5243, 2012

et al., 1999). Only quality assured, cloud screened, AERONET Level 2 data are used in this study to evaluate the MODIS aerosol product. To facilitate the comparison with MODIS, AERONET AOD measurements are interpolated to the 550 nm wavelength from multiple AEROENT wavelengths using a quadratic fit on a log-log scale (Eck et al., 1999).

2.2 Sea surface wind speed data

The Modern Era Retrospective-Analysis for Research and Applications (MERRA) meteorological database is used in the evaluation of the AOD retrieval uncertainty due to the surface wind speed assumption in the MODIS Ocean algorithm. MERRA has 1/2 degree latitude by 2/3 degree longitude resolution and provides an extensive source of meteorological variables (Rienecker et al., 2011). It uses the Goddard Earth Observing System-5 Data Assimilation System (GEOS-5 DAS) and a new set of physics packages for the atmospheric general circulation model (AGCM). The wind-related inputs into the MERRA system include wind speed data from Radiosondes, Pilot Balloon (PIBAL) measured winds, MODIS, Geostationary Operational Environmental Satellites (GOES), Special Sensor Microwave/Imager (SSM/I), Tropical Rainfall Measuring Mission (TRMM) Microwave Imager (TMI), NASA's Quick Scatterometer (QuickSCAT) and others. More information on the MERRA inputs can be found in the MERRA file specification document (http://gmao.gsfc.nasa.gov/merra/file_specifications.php). MERRA has been evaluated for accuracy and found to be one of the "best performing" reanalysis products for ocean surface turbulent flux and wind stress parameters (Brunke et al., 2011). Kennedy et al. (2011) show the MERRA near surface wind speeds to have biases within 0.5 $m\,s^{-1}$ when compared to the Atmospheric Radiation Measurement Program's (ARM) Cloud Modeling Best Estimate (CMBE) soundings during 1999–2001.

AMTD
5, 5205–5243, 2012

2.3 MODIS-AERONET collocation and coastal site classification

The spatially and temporally collocated MODIS and AERONET data pairs are acquired through the Multi-Sensor Aerosol Product Sampling System (MAPSS, http://giovanni.gsfc.nasa.gov/mapss/) (Ichoku et al., 2002; Petrenko et al., 2012). The database is a result of collocating the MODIS and AERONET measurements over the full record of MODIS spanning the years 2000-present and 2002-present (2010 for this study) for Terra and Aqua satellites, respectively. Two methods are used for collocating the MODIS and AERONET data. Firstly, AERONET measurements within ±30 min of the MODIS overpass time are averaged and compared against MODIS AOD retrievals averaged within a 55 km diameter centered over the AERONET sites (mean method, Ichoku et al., 2002). Using the mean method MAPSS also saves the mode of the quality flags from each pixel within the averaging region (55 km) to represent the quality flag for the collocated MODIS retrieval (Petrenko et al., 2012). Secondly, the MODIS AOD retrieval closest to the AERONET site is paired with the AERONET measurement that is closest to the MODIS overpass time (Central method). It is found here, as well as by Petrenko et al. (2012), that there is little difference between the central and mean methods, therefore, to be consistent with previous research and increase data volume the mean method is used for the remainder of this research.

Over the approximately 9 yr (2002–2010) record of Aqua-MODIS and AERONET AOD pairs, the result from the mean collocation method, that is consistent with Ichoku et al. (2002), shows that ∼ 26 % of the AERONET stations have MODIS retrievals from both the Land and Ocean algorithms, and consequently those sites are designated as coastal. All other AERONET sites are designated as non-coastal, being either Land only or Ocean only. The classification is done for all quality flag cases as well as for the quality flag filtered (Ocean flag greater than 0, Land flag 3) data set. The classification shows little variation between each method, thus to remain consistent we use the best quality flag classification.

AMTD
5, 5205–5243, 2012

3 MODIS overall performance in coastal vs. non-coastal regions

The MODIS-AERONET pairs are examined on a global scale and split into three categories. The first includes all AERONET sites (global), the second consists of only coastal AERONET sites (coastal), and the third is made up of only non-coastal sites (non-coastal). We utilize multiple metrics to statistically evaluate the MODIS AOD accuracy with respect to AOD measured by AERONET.

3.1 Metrics for comparing MODIS and AERONET AOD

The first type of metric is a combination of parameters that are commonly used to describe the relationship between two variables including: bias, mean, standard deviation, correlation, statistical significance, and best-fit (ordinary-least-square) regressions. MODIS AOD bias is calculated by subtracting AERONET AOD from the paired MODIS AOD, and then averaging each pair for all AERONET sites for the full time period ~2002–2010 to obtain the mean bias for each site. In addition, the biases are calculated for the Land, Ocean and Land_and_Ocean products, respectively. Global plots are then created to reveal the MODIS bias along the coast. Furthermore, the correlation, variance and root mean square difference (RMSD) between MODIS AOD and AERONET AOD are combined to generate the well known Taylor Diagram to aid the visualization of the differences found in the comparison. Designed by Taylor (2001), the Taylor Diagram uses a 2-D polar plot to demonstrate three pieces of information that are interconnected, in which radius represents normalized standard deviations, cosine of the angle represents correlation, and the radius of the circles centered on point "REF" (e.g. radius of 1) along the x-axis indicates normalized RMSD. As will be shown in Sect. 3.2, the Taylor Diagram is particularly useful for visualizing the error characteristics of each of the MODIS aerosol algorithms over varying surface types.

While the first type of metric is useful, it may not be sufficient to fully describe the goodness of fit between two data sets, especially when the population in the datasets are not normally distributed (Wilks, 2011). In other words, statistically significant

AMTD
5, 5205–5243, 2012

correlation and/or small bias does not necessarily warrant that the fitness between the two datasets is statistically significant. As shown in Fig. 1, the AOD frequencies over coastal sites (and non-coastal sites, not shown) are not normally distributed; indeed, they are log-normal (Fig. 2), which is consistent with previous studies (O'Neill et al., 2000). Note that the MODIS Land algorithm allows negative values when retrieving AOD. From 2002–2010 approximately 400 retrievals from MODIS when paired with AERONET over the coastal regions resulted in negative AODs and those retrievals are not included in the analyses presented in this paper. Two parameters, μ and σ, represent the location parameter and scale parameter respectively, and can be identified to fully describe a log-normal probability density function (PDF). Where μ is the mean of the logarithm of AODs, and σ is the standard deviation of the logarithm of AODs. The actual frequency for AOD values between τ and $\tau + \Delta\tau$ can be obtained by integrating the PDF over the range τ to $\tau + \Delta\tau$, and then multiplying the integral by the total number of sample data points.

To evaluate if the (log-normal) PDFs of MODIS AOD data fit with that of the AERONET measurements at a statistically significant level, a second type of statistic metric is used that consists of a t-test for difference of mean for paired data, a likelihood ratio test, and a Kolmogorov-Smirnov (K-S) test. Briefly, after the difference (e.g. bias) in each data pair is computed, the mean difference (or mean bias) can be estimated and then compared with the difference between the means for each variable (e.g. MODIS AOD or AERONET AOD), μ_Δ. The t-test for statistical significance is then applied to $z = \frac{\bar{\Delta} - \mu_\Delta}{(s_\Delta^2/n)^{1/2}}$, where s_Δ^2 is the sample variance of the Δ_i differences for a total of n pairs (Wilks, 2011). A very small p-value (less than 0.01) indicates at which statistically significant level (99 %) that the null hypothesis is not true, or the difference between means for the paired data is significant.

A likelihood ratio test is a parametric test to determine the likelihood that the MODIS derived AODs could have been drawn from the same log-normal distribution as the AERONET AODs. To perform this test it is necessary to fit

AMTD
5, 5205–5243, 2012

log-normal distributions separately to each MODIS algorithm and AERONET, and compare these two distributions with the single log-normal distribution fit using both sets of data (Wilks, 2011). The general form of the likelihood test statistic is $\varphi^* = 2 \cdot \ln\left[\frac{\varphi(H_A)}{\varphi(H_0)}\right] = 2 \cdot \left[L(H_A) - L(H_0)\right]$, where $\varphi(H_A)$ and $\varphi(H_0)$ are the likelihood functions and L is the log-likelihood. For our case the test statistic is equal to $\varphi^* = 2 \cdot \left\{\left[\sum_{i=0}^{\tau} \mathrm{PDF}_{\mathrm{MODIS}}\right] + \left[\sum_{i=0}^{\tau} \mathrm{PDF}_{\mathrm{AERONET}}\right] - \left[\sum_{i=0}^{\tau} \mathrm{PDF}_{\mathrm{MODIS\ and\ AERONET}}\right]\right\}$, where the PDFs are a function of μ, σ, and τ. Since there are 4 parameters used to estimate the individual AERONET and MODIS distributions and 2 for the null hypothesis that MODIS and AERONET AOD data are from the same PDF ($\mathrm{PDF}_{\mathrm{MODIS\ and\ AERONET}}$), φ^* is evaluated with the χ^2 table for degrees of freedom (of $\nu = 2$).

The K-S test compares the cumulative density functions (CDFs, integral of PDFs) of each of the MODIS algorithms to that of AERONET. The test statistic is represented by the maximum difference between the MODIS and AERONET CDFs, $D = \max|\mathrm{CDF}_{\mathrm{MODIS}} - \mathrm{CDF}_{\mathrm{AERONET}}|$. When D is greater than the critical value, $1.36/\sqrt{n}$, the null hypothesis that the two CDFs show a good fit is rejected at the 99 % confidence level. By analyzing the fitness between the MODIS and AERONET PDFs and CDFs, our evaluation goes beyond the bias and correlation tests that have been used commonly in the past to evaluate MODIS AOD accuracy, and hence provides a more robust statistical technique that is needed to move toward a more complete description of the uncertainty in MODIS AOD retrievals.

3.2 Coastal vs. non-coastal MODIS AOD evaluation

Although previous MODIS analysis, over a global average, was valuable for understanding MODIS error characteristics (Kahn et al., 2011, 2007, 2005; Levy et al., 2007a, 2010; Mi et al., 2007; Remer et al., 2005; and others), an examination of coastal regions shows a reduction in MODIS accuracy. Shown in Fig. 1 are the AOD frequencies for each of the MODIS algorithms and the AERONET measurements over coastal

AMTD
5, 5205–5243, 2012

regions. It is visible that the distributions are not Gaussian. Indeed, a log-normal distribution is found for MODIS and AERONET AODs over the coastal, non-coastal (not shown), and global stations (not shown), and the corresponding parameters (μ, σ) for coastal retrievals are shown in Fig. 1 with the PDFs shown in Fig. 2. Using a χ^2 test we find that the log-normal PDFs fit each distribution at a statistically significant level (Fig. 2).

After quality flag filtering, MODIS reported AODs are highly correlated with the paired AOD from AERONET with R^2 of 0.8, regardless if AODs are retrieved over costal or non-costal region (respectively shown in top-row and bottom row in Fig. 3), and/or from Ocean algorithm, Land algorithm, and Ocean_and_Land combined (respectively shown in three columns in Fig. 3). Compared with AERONET AOD, MODIS AOD retrievals from the Ocean algorithm have a correlation coefficient (R^2) of 0.809 and a regression equation of $\tau_M = 0.913 \cdot \tau_A + 0.028$ (where subscripts A and M represent AERONET and MODIS, respectively) at global scale (figure not shown), R^2 of 0.804 and $\tau_M = 0.863 \cdot \tau_A + 0.034$ for all the coastal sites (Fig. 3f), and a larger R^2 of 0.854 and $\tau_M = 1.115 \cdot \tau_A - 0.001$ for all non-coastal (e.g. open ocean) sites (Fig. 3c). In comparison, MODIS AODs from the Land algorithm show an R^2 of 0.793 and linear regression $\tau_M = 0.979 \cdot \tau_A + 0.008$ for all AERONET stations (figure now shown), R^2 of 0.795 and $\tau_M = 1.027 \cdot \tau_A + 0.016$ for coastal stations (Fig. 3e), and R^2 of 0.795 and $\tau_M = 0.971 \cdot \tau_A + 0.004$ for non-coastal (inland) sites (Fig. 3b). In contrast to the Ocean algorithm AOD, there seems to be little change in correlation between the coastal, non-coastal and global evaluations of the Land algorithm AOD. However, the Ocean AOD correlation is consistently greater than the Land AOD correlation in all the respective categories.

Figure 3 also shows that the AODs over coastal and non-coastal regions retrieved from the Land algorithm both fall within the expected error (EE) envelope greater than 66 % of the time (Fig. 3b, e), but the counterparts from Ocean algorithm only fall within the EE envelope ~58 % of time, which is lower than 66 % that is revealed from the past studies of MODIS *collection 4* that don't separate the AERONET-MODIS AOD comparisons into coastal and non-coastal regions (Remer et al., 2005). Nevertheless,

AMTD
5, 5205–5243, 2012

while the EE for Ocean algorithm is smaller than that for Land algorithm, the bias is found to be less (Fig. 3).

Figure 3 shows that a small bias (often < 0.03) of AOD overall is consistent with past research (Levy et al., 2010; Remer et al., 2005), but for the same type of product (e.g. from Ocean algorithm, Land algorithm, and combined Land_and_Ocean), a larger bias of AOD is apparent over the coastal regions than over non-coastal regions (Fig. 3d–f). It is noted that for AOD from the Ocean algorithm, the overall bias (0.012) along the coast is larger than the counterparts (0.006) over the open ocean (Fig. 3f vs. c). Although, this is a bit misleading because of two counteracting effects over the coast where AOD larger than 0.25 are underestimated by 0.029 whereas those smaller than 0.25 are overestimated by 0.021 (Table 1). The AOD value of 0.25 was chosen as the cutoff because Levy et al. (2010) suggest that regardless of quality flag, AOD less than 0.2 may represent an aerosol signal that is too low to retrieve meaningful aerosol size information from MODIS. Using a t-test for difference we find that regardless of the MODIS product (i.e., Ocean, Land, Land_and_Ocean), the AOD bias over coastal regions are statistically significant beyond the 99 % confidence level with a p-value much less than 0.01. In order to gain insight into the locality of the over- and under-estimation, a plot of bias at different coastal stations is shown in Fig. 4.

It is demonstrated in Fig. 4 that the Land algorithm has a significantly larger bias than the Ocean algorithm for most coastal AERONET sites. This is expected because of the inherent difficulties in characterizing land surfaces in general. The average MODIS AOD bias for the Land algorithm over coastal sites is 0.026 and shows little dependence on AOD amount (Table 1); again using a t-test for difference we find p-values much less than 0.01 revealing that the bias in AOD retrieval from the Land algorithm is statistically significant. However, the bias results show large variation amongst different coastal AERONET sites (Fig. 4).

The Taylor Diagram (Fig. 5) visualizes the overall performance of the MODIS aerosol algorithms in a single figure. The MODIS correlation coefficient with AERONET visibly decreases for coastal retrievals compared to non-coastal retrievals, with R^2-values of

AMTD
5, 5205–5243, 2012

0.795 (for AOD from Land algorithm) to 0.818 (for AOD from Ocean algorithm) over the coast compared to the corresponding R^2-values of 0.795 (Land) to 0.854 (Ocean) for non-coastal regions (Fig. 5). Furthermore, the normalized standard deviations of MODIS AOD increase from roughly 0.8 for non-coastal retrievals to 1.3 for coastal retrievals (Fig. 5), indicating that MODIS AOD is less capable of capturing the temporal variation of AERONET AOD over the coastal sites. By the same token, Fig. 5 also demonstrates that the Ocean algorithm over the open-ocean (non-coastal) captures the variation in AOD better than the other algorithms, because its resultant representation in the Taylor diagram is closest to the point "REF" indicating the best performance with respect to AERONET. It is shown that all of the MODIS AOD retrievals over the coast, regardless of algorithm, cluster farthest away from the "REF" point, indicating a need for refinement of the MODIS product over coastal regions (Fig. 5).

To further evaluate if MODIS aerosol products represent the statistics observed from AERONET, the PDFs from the MODIS products are used to compare against the PDF from AERONET to determine the fitness of the AOD frequencies. The t-test for difference of mean, described in Sect. 3.1, reveals p-values of much less than 0.01 for the difference of each of the MODIS AOD products to AERONET, demonstrating that at a statistically significant level the mean of MODIS AOD products are different from the mean of paired AERONET AOD over the coast. Going beyond the t-test for difference of mean we apply the likelihood ratio test and the K-S test for goodness-of-fit.

The likelihood test returns a test statistic φ as described in Sect. 3.1. The test statistic is compared to a critical value to determine the likelihood that the MODIS AOD PDF fits the PDF from AERONET AOD. The critical value for the χ^2 statistics with $\nu = 2$ degrees of freedom at the 99 % confidence level is 9.210, where anything greater than this value results in rejecting the null hypothesis that the PDFs may come from the same distribution. We find that the test statistics are 23.03, 29.77, and 22.98 for the quality filtered MODIS Land, Ocean, and Land_and_Ocean products, respectively. Therefore, we conclude that the PDFs from the MODIS algorithms statistically differ from the PDFs from AERONET over coastal regions. This finding indicates that MODIS is not very

AMTD
5, 5205–5243, 2012

accurate in modeling the actual nature as represented by AERONET. The likelihood test is useful to compare PDFs. However, to more fully describe the fitness between MODIS and AERONET data, our analysis is extended to CDFs as well.

Figure 6 displays the results of the K-S test and maximum difference for the CDFs from each quality filtered MODIS algorithms to the CDF from AERONET. The critical values (described in Sect. 3.1) needed to conclude that the MODIS Land, Ocean, and Land_and_Ocean AOD CDFs fit the counterpart of the AERONET AOD, at a 99 % confidence level, are respectively 0.013, 0.009, and 0.008 (Fig. 6). If the difference is greater than the respective critical values then the null hypothesis (CDF from MODIS AOD fit with CDF from AERONET AOD) must be rejected and the CDFs are significantly different. It is clear in Fig. 6 that the maximum departures of the CDFs from each of the MODIS AOD products and AERONET AOD observation are greater than the corresponding critical values (Fig. 6). Therefore, it is concluded that the CDFs from each of the MODIS algorithms do match the AERONET CDF at a statistically significant level; in fact, they differ at beyond the 99 % confidence level. This only strengthens the finding from the previous tests that MODIS does not model the actual nature represented by the AEROENT AOD observations.

4 Impact of quality filter for the Land_and_Ocean AOD

The Land_and_Ocean data set is created by combining (a simple union) retrievals from the MODIS Land algorithm and the MODIS Ocean algorithm to provide a more complete spatial coverage of AOD over the globe. However, unlike the Land dataset and the Ocean dataset, the combined dataset is not assigned a specific quality flag. For the purposes of this work, the combined retrievals were considered “high quality” if either the mode of the corresponding Land flag is equal to 3 or the mode of the Ocean flag is greater than 0. The meaning of each quality flag category is explained above in Sect. 2. Note that mean AOD calculated from the Land_and_Ocean dataset may not be equal to the mean AOD calculated from the separate Land or Ocean datasets because

AMTD
5, 5205–5243, 2012

the mean of the Land_and_Ocean product within the 55 km region around AERONET may include MODIS pixels originating from either (or both) the Ocean and Land algorithms. Because the AOD pixels from the Land algorithm are different than those from the Ocean algorithm they might represent completely different aerosols only further complicating the Land_and_Ocean analysis.

The QA filtering as described above improves the global MODIS Land_and_Ocean correlation (R^2) with AERONET from 0.737 to 0.804 (figure not shown), and reduces the AOD bias by 34 % for coastal regions from 0.029 to 0.019 (Table 1). Focusing on the high AOD events (AOD > 0.25) over the coast reduces the bias even more, at 62 % from 0.026 to 0.010 (Table 1). Bias values were evaluated using a t-test for difference and are found to have p-values much less than 0.01 and, therefore, are still statistically significant. However, the number of MODIS-AERONET pairs is reduced from 113 152 to 71 303 globally (or by 37 %) after applying the quality flag filter. The Land_and_Ocean, quality assured, data set has an R^2 of 0.804 and a regression equation of $\tau_M = 0.964 \cdot \tau_A + 0.014$ on a global scale over the full record of MODIS (figure not shown), and over coastal regions has an R^2 of 0.818, and a regression of $\tau_M = 0.933 \cdot \tau_A + 0.028$ (Fig. 3). Furthermore, the t-test for difference reveals that the closest or statistically best fit to the AERONET data over the coast is observed from the quality filtered Land_and_Ocean product, with p-values changing from $\sim 1 \times 10^{-5}$ to $\sim 1 \times 10^{-6}$ after the filter. The reduction in bias from the quality filter can be observed in Fig. 4d vs. 4e and an increase in correlation is found on a global scale. However, even after the quality flag filter, the coastal regions still show poorer MODIS performance compared to the non-coastal retrievals (Fig. 5). The result suggests that a dedicated algorithm for coastal retrievals may be needed in lieu of the current Land and Ocean algorithms used for MODIS aerosol retrievals.

AMTD
5, 5205–5243, 2012

5 Wind and cloud impact on the MODIS ocean algorithm

Different sources of error arise in the MODIS Ocean retrievals because of surface characteristic assumptions made to create the LUTs used by the algorithm, and the validity of a pixel for the AOD retrieval depends on the result of cloud-mask algorithm designed specifically for the MODIS Ocean product. We examine the sources of error separately to more accurately describe the MODIS performance over the coastal regions. We focus on the possible cloud contamination described by Zhang and Reid (2006) and the surface wind speed assumption of $6\,m\,s^{-1}$ in the MODIS Ocean algorithm.

It is known that cloud contamination can affect MODIS AOD accuracy over the ocean (Zhang and Reid, 2006) for the *collection 4* product. However, the virtue of AERONET QA screening collocated MODIS-AERONET retrievals are biased toward the cloud-free scenes (Smirnov et al., 2011). We investigate the possible cloud contamination for the *collection 5.1* MODIS product for coastal waters by using the MODIS reported cloud fraction for over ocean retrievals. Multiple thresholds for cloud fraction are tested and Table 2 contains results from the 80 % threshold, 70 % threshold, and the standard quality flag filtered MODIS product. The threshold analysis reveals that the 70 % threshold can greatly reduce bias while maintaining a sufficient number of retrievals, with a reduction of only 16 % globally and 14 % over coastal regions (Table 2). For the cloud fraction threshold of 70 % (80 %) the reduction of bias for coastal sites is 100 % (67 %) and for non-coastal sites is 58 % (33 %) (Table 2). At first glance it may seem the filter removes all bias from coastal retrievals, however, this is not the case. MODIS bias for AOD events greater than 0.25 actually increases by 21 % for both the 80 % and 70 % cloud fraction filters.

While Table 2 shows consistent results with Zhang and Reid (2006) that the removal of MODIS over-ocean AODs where pixels correspond to a cloud fraction larger than a threshold of 80 % can significantly reduce the errors in AOD estimates, a more detailed examination also shows that the cloud fraction filter leads to an even more negative bias for AOD events over 0.25 and reduces the positive bias for AOD events

AMTD
5, 5205–5243, 2012

less than 0.25 (Table 2). Zhang and Reid (2006, 2010) demonstrate that the cloud contamination causes MODIS overestimation due to the high reflectivity of clouds in the visible spectrum, and therefore, filtering AOD retrievals by cloud fraction would lead to an overall decrease in MODIS AOD. The same physical interpretation is true for MODIS collection 5.1; however, the negative bias persistent for AOD over 0.25 requires another explanation.

In addition to cloud contamination, error may be introduced into the MODIS Ocean algorithm by inherent assumptions in calculating the LUTs, specifically, the surface wind speed of $6\,m\,s^{-1}$ (Kleidman et al., 2012; Zhang and Reid, 2010; Shi et al., 2011). Kleidman et al. (2012) show a systematic increase of MODIS error as a function of wind speed for retrievals over the open-ocean. This dependence is most apparent when wind speed deviates from the $6\,m\,s^{-1}$ speed assumed for the rough ocean surface and white cap parameterizations within the MODIS AOD retrievals (Kleidman et al., 2012). To our knowledge, the impact of varying wind speeds on the MODIS retrieval accuracy over coastal waters has not been studied, although previous work on wind climatologies suggests that surface wind speeds over coastal regions are frequently slower than $6\,m\,s^{-1}$ (Lavagnini et al., 2005; Martin et al., 1999; Maryland Department of Natural Resources, 2011). To quantify the impact of the surface wind speed on coastal aerosol retrievals, we stratify the analysis of MODIS-AERONET biases (before and after cloud-contamination filtering) as a function of ocean surface wind speed. At every coastal AERONET site, each MODIS AOD bias is paired spatially and temporally with the corresponding 2-m wind speed from the MERRA re-analysis.

We first conduct the correlation analysis for MERRA 2-m wind speed and the bias in MODIS AOD without filtering by cloud fraction (but with QA flag assured). A positive correlation between wind speed and MODIS AOD bias for all coastal sites is shown in Fig. 7, with a linear best fit of $\tau_{bias} = 0.010 \cdot v - 0.020$ before cloud filtering, where τ_{bias} is MODIS AOD bias and v is wind speed. The positive correlation between bias and wind speed can be understood from the following two factors: (1) wind speeds over coastal regions are frequently (94 % of the time) less than $6\,m\,s^{-1}$ at the time of

AMTD
5, 5205–5243, 2012

MODIS retrievals (Fig. 8b), and (2) slower wind speeds lead to more negative MODIS bias while faster wind speeds lead to positive bias (Fig. 8a). While factor (1) explains, in part, the negative bias for the AOD (greater than 0.25) retrieved from the Ocean algorithm, factor (2) can be used to interpret the overestimation in MODIS AOD for AOD less than 0.25 over the coast. High AOD near the coast may occurs during high wind conditions that can generate more sea salt particles or can be associated with frontal passage moving aerosols from land to ocean; in either case, such high winds, if they're larger than $6\,\mathrm{m\,s^{-1}}$, can lead to overestimation in MODIS AOD retrievals. This effect on MODIS retrievals needs to be studied in future research. However, with the known impact of cloud contamination, we conduct a similar analysis after filtering out the retrievals with cloud fractions greater than 70 %.

The linear regression equation between wind speed and MODIS bias, after accounting for cloud contamination (Fig. 8c), is then used as an empirical correction for the MODIS Ocean algorithm retrievals over the coast. The linear regression found for the MODIS bias dependence on wind speed is $\tau_{\mathrm{bias}} = 0.010 \cdot v - 0.024$, after applying the 70 % cloud fraction (Fig. 8c). By including the wind speed at the time of each MODIS AOD retrieval, we can estimate the MODIS bias by using the τ_{bias} equation and subtract it from the MODIS-retrieved AOD to improve the AOD retrieval accuracy. The empirical correction yields a reduction in overall MODIS AOD bias for the Ocean algorithm over the coast from +0.006 for the standard quality flag filtered MODIS product to −0.0005 for the cloud and wind corrected AOD. Furthermore, for AOD events less than 0.25 the bias is reduced from +0.021 to +0.0098, and for AOD events greater than 0.25 the bias is reduced from −0.029 to −0.027. The success of the correction scheme suggests that bias introduced into AOD retrievals by wind speed assumptions can be reduced by using real or modeled wind speed data. Along with the reduced bias, the correlation and best fit regression show a better fit to the AERONET AOD data for the corrected results when compared to the original MODIS Ocean product (Fig. 5). Figure 5 is particularly useful for observing the benefits from the correction scheme because it shows the shift (represented by the black arrow) from the QA flag assured

AMTD
5, 5205–5243, 2012

Ocean product to the corrected Ocean product. From Fig. 5 it is immediately clear that the corrections improves the MODIS AOD correlation with AERONET and reduces the variance in observation, indicating that the temporal variation is better captured by the corrected product. Furthermore, after both cloud and wind correction the MODIS frequency shows a better fit to the AERONET distribution than the standard MODIS Ocean product (Fig. 8). Although the corrected MODIS AOD CDF does not pass the K-S test with a maximum difference of 0.024 and a critical value of 0.011 at the 99 % confidence level, the correction does show an improvement with a reduction in the maximum difference from the AERONET CDF over the standard MODIS product and the cloud fraction filter alone (Fig. 9).

For high AOD events (greater than 0.25) the MODIS bias is reduced by applying the empirical wind speed correction. However, because the cloud fraction filter results in a more negative trend to the already negative MODIS bias, the wind speed correction is less visible. A possible cause of the more negative bias after cloud filtering is that cloud contamination has a greater influence, proportionally, on lower AOD retrievals than on higher AODs. The increased reflection from cloud contamination has a proportionally reduced impact on total reflection (Kleidman et al., 2012). Thus, the cloud contamination filter removes some of the high AOD events that are minimally impacted by high cloud fractions, and may skew the results to a more negative bias. This impact will be evaluated in future studies.

An assessment of the covariance between cloud fraction and wind speed is provided in Fig. 8d. The scatter plot of wind speed and cloud fraction for coastal retrievals clearly shows that the wind speed and cloud fraction are not correlated (Fig. 8d) and, therefore, a correction scheme that accounts for each independently, such as above, is an appropriate method.

To further evaluate the effectiveness of our empirical method to correct the AOD bias due to assumed weed speed in the MODIS algorithm, we show the correlation between the MERRA 2-m wind speed and MODIS AOD bias, as well as the slope and intercept from the best linear fit between the two at each coastal AERONET site. It

AMTD
5, 5205–5243, 2012

is visible that 46 out of the possible 62 coastal AERONET sites show a statistically significant correlation between MODIS bias and wind speed (Fig. 7b). Furthermore, from those statistically significant sites, 40 are found to have a negative MODIS bias as the wind speed approaches zero (Fig. 7c), and 45 are found to have a regression with a positive slope that indicates a systematic positive bias in MODIS AOD as wind speeds increase (Fig. 7d). Due to the high proportion of sites showing a statistically significant dependence to wind speed, a generalization can be extended to all coastal sites.

6 Conclusions and discussion

Approximately 9 yr of Aqua-MODIS aerosol retrievals are evaluated using AEROENT aerosol measurements for validation. Specific focus in the analysis is given to the coastal regions of the world due to their complex surface characteristics and the dominant contribution to the loading of anthropogenic aerosols in the atmosphere. Over the coast the MODIS aerosol algorithms show increased uncertainty with respect to non-coastal regions.

After filtering by quality flags, the MODIS AODs respectively retrieved from the Land and Ocean algorithms are highly correlated with AERONET (with $R^2 \approx 0.8$), but only the Land algorithm AODs fall within the expected error envelope greater than 66 % of the time. Furthermore, MODIS AODs after quality flag filtering, regardless from Land algorithm, Ocean algorithm, or combined Land_and_Ocean product, show statistically significant discrepancy with their respective counterparts from AERONET in terms of mean, probability density function, and cumulative density function, which suggest the need for improvement in coastal retrieval algorithms.

The MODIS over ocean algorithm is found to have two major sources of error over coastal regions. The first is cloud contamination that leads to an overestimation of AOD, and this result is in agreement with Zhang and Reid (2006, 2010) in their global MODIS AOD analysis that did not segregate between coastal and non-coastal sites.

AMTD
5, 5205–5243, 2012

The second source of error is dependent on near surface wind speed due to the assumptions made in the MODIS AOD retrievals over ocean. Based upon MERRA data, we found that wind speeds over the coastal ocean are frequently slower than the $6\,m\,s^{-1}$ assumed by the MODIS Ocean algorithm. This high bias in wind speed pre-described in the MODIS Ocean algorithm often leads to an overestimation of the surface reflectance contribution to the radiance measured by the satellite at the top of atmosphere and so an underestimation of the aerosol reflectance contribution, leading to an underestimation of AOD. After applying the equation $\tau_{bias} = 0.010 \cdot v - 0.024$, where τ_{bias} is estimated MODIS bias and v is surface wind speed, to the MODIS AOD retrievals from the Ocean algorithm, the corresponding MODIS AODs are in better agreement with paired AEROENT AODs, which should be useful for future analysis of AOD trend and MODIS AOD data assimilation.

Acknowledgements. Funding for this research was provided by NASA GSFC, NASA Nebraska Space Grant Consortium, and the Department of Earth and Atmospheric Sciences at the University of Nebraska-Lincoln. J. Wang also acknowledges the NASA Radiation Science Program and Atmospheric Composition and Analysis Program for support. We are grateful to Brent Holben, all investigators, and support staff associated with AERONET. Special thanks are extended to Scott Mellor for helping edit the manuscript, and Robert C. Levy for his insights on how ocean pixels are treated in the MODIS aerosol algorithm over land. Our final thought is for Gregory Leptoukh who tragically passed away during this research. Without his vision and foresight this project would have never been possible.

References

Bhaskaran, S., Neal, P., Rahman, A., and Mallick, J.: Applications of Satellite Data for Aerosol Optical Depth (AOD) retrievals and validation with AERONET data, Atmospheric and Climate Sciences, 01, 61–67, doi:10.4236/acs.2011.12007, 2011.

Bréon, F., Vermeulen, A., and Descloitres, J.: An evaluation of satellite aerosol products against sunphotometer measurements, Remote Sens. Environ., online first: doi:10.1016/j.rse.2011.06.017, 2011.

AMTD
5, 5205–5243, 2012

Brunke, M., Wang, Z., Zeng, X., Bosilovich, M., and Shie, C.-L.: An assessment of the uncertainties in ocean surface turbulent fluxes in 11 reanalysis, satellite-derived, and combined global datasets, J. Climate, 24, 5469–5493, doi:10.1175/2011JCLI4223.1, 2011.

Charlson, R., Shwartz, S., Hales, J., Cess, R. D., Coakley Jr., J. A., Hansen, J. E., and Hofmann, D. J.: Climate forcing by anthropogenic aerosols, Science, 255, 423–430, 1992.

Chatterjee, A., Michalak, A. M., Kahn, R., Paradise, S. R., Braverman, A. J., and Miller, C. E.: A geostatistical data fusion technique for merging remote sensing and ground-based observations of aerosol optical thickness, J. Geophys. Res., 115, 1–12, doi:10.1029/2009JD013765, 2010.

Cox, C. and Munk, W.: Statistics of the sea surface derived from sun glitter, Journal Maritime Science, 13, 198–227, 1954.

Eck, T., Holben, B., Reid, J., Dubovik, O., Smirnov, A., O'Neill, N. T., Slutsker, I., and Kinne, S.: Wavelength dependence of the optical depth of biomass burning, urban, and desert dust aerosols, J. Geophys. Res., 104, 333–349, doi:10.1029/1999JD900923, 1999.

Holben, B., Eck, T., Slutsker, I., Tanre, D., Buis, J. P., Setzer, A., Vermote, E., Reagan, J. A., Kaufman, Y. J., Nakahima, T., Lavenu, F., Jankowiak, I., and Smirnov, A.: AERONET – a federated instrument network and data archive for aerosol characterization, Remote Sens. Environ., 66, 1–16, 1998.

Ichoku, C., Chu, D., Mattoo, S., Kaufman, Y. J., Remer, L. A., Tanre, D., Slutsker, I., and Holben, B. N.: A spatio-temporal approach for global validation and analysis of MODIS aerosol products, Geophys. Res. Lett., 29, 1–4, doi:10.1029/2001GL013206, 2002.

Kahn, R. A., Gaitley, B. J., Martonchik, J. V., Diner, D. J., Crean, K. A., and Holben, B.: Multiangle Imaging Spectroradiometer (MISR) global aerosol optical depth validation based on 2 years of coincident aerosol robotic network (AERONET) observations, J. Geophys. Res., 110, 1–16, doi:10.1029/2004JD004706, 2005.

Kahn, R. A., Garay, M. J., Nelson, D. L., Yau, K. K., Bull, M. A., Gaitley, B. J., Martonchik, J. V., and Levy, R. C.: Satellite-derived aerosol optical depth over dark water from MISR and MODIS: comparisons with AERONET and implications for climatological studies, J. Geophys. Res., 112, D18205, doi:10.1029/2006JD008175, 2007.

Kahn, R. A., Garay, M. J., Nelson, D. L., Levy, R. C., Bull, M. A., Diner, D. J., Martonchik, J. V. Hansen, E. G., Remer, L. A., and Tanre, D.: Response to "Toward unified satellite climatology of aerosol properties. 3. MODIS versus MISR versus AERONET", J. Quant. Spectrosc. Ra., 112, 901–909, doi:10.1016/j.jqsrt.2010.11.001, 2011.

AMTD
5, 5205–5243, 2012

Kaufman, Y. J., Tanre, D., Remer, L. A., Vermote, E. F., Chu, A., and Holben, B. N.: Operational remote sensing of tropospheric aerosol over land from EOS moderate resolution imaging spectroradiometer, J. Geophys. Res., 102, 17051–17067, 1997.

Kennedy, A., Dong, X., Xi, B., Xie, S., Zhang, Y., and Chen, J.: A comparison of MERRA and NARR reanalyses with the DOE ARM SGP data, J. Climate, 24, 4541–4557, doi:10.1175/2011JCLI3978.1, 2011.

Kinne, S., Lohmann, U., Feichter, J., Schulz, M., Timmreck, C., Ghan, S., Easter, R., Chin, M., Ginoux, P., Takemura, T., Tegen, I., Koch, D., Herzog, M., Penner, J., Pitari, G., Holben, B., Eck, T., Smirnov, A., Dubovik, O., Slutsker, I., Tanre, D., Torres, O., Mishchenko, M., Geogdzhayev, I., Chu, D. A., and Kaufman, Y.: Monthly averages of aerosol properties: a global comparison among models, satellite data, and AERONET ground data, J. Geophys. Res., 108, 4634, doi:10.1029/2001JD001253, 2003.

Kleidman, R., Smirnov, A., Levy, R. C., Mattoo, S., and Tanre, D.: Evaluation and wind speed dependence of MODIS aerosol retrievals over open ocean, IEEE T. Geosci. Remote, 50, 429–435, doi:10.1109/TGRS.2011.2162073, 2012.

Koepke, P.: Effective reflectance of oceanic whitecaps, Appl. Optics, 23, 1816–1824, 1984.

Lavagnini, A., Sempreviva, A., Transerici, C., Accadia, C., Casaioli, M., Mariani, S., and Spreanza, A.: Offshore wind climatology over the Mediterranean basin, Wind Energy, 9, 251–266, doi:10.1002/we.169, 2005.

Levy, R. C., Remer, L. A., Martins, J. V., Kaufman, Y. J., Plana-Fattori, A., Redemann, J., and Wenny, B.: Evaluation of the MODIS Aerosol Retrievals over Ocean and Land during CLAMS, J. Atmos. Sci., 62, 974–992, doi:10.1175/JAS3391.1, 2005.

Levy, R. C., Remer, L., and Dubovik, O.: Global aerosol optical properties and application to moderate resolution imaging spectroradiometer aerosol retrieval over land, J. Geophys. Res., 112, 1–15, doi:10.1029/2006JD007815, 2007a.

Levy, R. C., Remer, L. A., Mattoo, S., Vermote, E. F., and Kaufman, Y. J.: Second-generation operational algorithm: retrieval of aerosol properties over land from inversion of moderate resolution imaging spectroradiometer spectral reflectance, J. Geophys. Res., 112, 1–21, doi:10.1029/2006JD007811, 2007b.

Levy, R. C., Remer, L. A., Kleidman, R. G., Mattoo, S., Ichoku, C., Kahn, R., and Eck, T. F.: Global evaluation of the Collection 5 MODIS dark-target aerosol products over land, Atmos. Chem. Phys., 10, 10399–10420, doi:10.5194/acp-10-10399-2010, 2010.

AMTD
5, 5205–5243, 2012

Martín, M., Cremades, L., and Santabàrbara, J.: Analysis and modeling of time series of surface wind speed and direction, Int. J. Climatol., 19, 197–209, 1999.
Maryland Department of Natural Resources: Maryland Offshore Wind Climatology with Application to Wind Power Generation 21 January 2011, State Report, 2011.
Mi, W., Li, Z., Xia, X., Holben, B., Levy, R., Zhao, F., Chen, H., and Cribb, M.: Evaluation of the moderate resolution imaging spectroradiometer aerosol products at two aerosol robotic network stations in China, J. Geophys. Res., 112, 1–14, doi:10.1029/2007JD008474, 2007.
Mishchenko, M. and Geogdzhayev, I.: Satellite remote sensing reveals regional tropospheric aerosol trends, Opt. Express, 15, 7423–7438, doi:10.1364/OE.15.007423, 2007.
Mishchenko, M., Geogdzhayev, I., Rossow, W., Cairns, B., Carlson, B. E., Lacis, A. A., Liu, L., and Travis, L. D.: Long-term satellite record reveals likely recent aerosol trend, Science, 315, 1534, doi:10.1126/science.1136709, 2007.
Myhre, G.: Consistency between satellite-derived and modeled estimates of the direct aerosol effect, Science, 324, 187–190, doi:10.1126/science.1174461, 2009.
O'Neill, N. T., Ignatov, A., Holben, B. N., and Eck, T. F.: The lognormal distribution as a reference for reporting aerosol optical depth statistics; empirical tests using multi-year, multi-site AERONET sunphotometer data, Geophys. Res. Lett., 27, p. 3333, doi:10.1029/2000GL011581, 2000.
Petrenko, M., Ichoku, C., and Leptoukh, G.: Multi-sensor Aerosol Products Sampling System (MAPSS), Atmos. Meas. Tech., 5, 913–926, doi:10.5194/amt-5-913-2012, 2012.
Remer, L. A., Kaufman, Y. J., Tanre, D., Mattoo, S., Chu, D. A., Martins, J. V., Li, R.-R., Ichoku, C., Levy, R. C., Kleidman, R. G., Eck, T. F., Vermote, E., and Holben, B. N.: The MODIS aerosol algorithms, products, and Validation, J. Atmos. Sci., 62, 947–973, doi:10.1175/JAS3385.1, 2005.
Remer, L. A., Kleidman, R. G., Levy, R. C., Kaufman, Y. J., Tanre, D., Mattoo, S., Martins, J. V., Ichoku, C., Koren, I., Yu, H., and Holben, B. N.: Global aerosol climatology from the MODIS satellite sensors, J. Geophys. Res., 113, 1–18, doi:10.1029/2007JD009661, 2008.
Rienecker, M. M., Suarez, M. J., Gelaro, R., Todling, R., Bacmeister, J., Liu, E., Bosilovich, M. G., Schubert, S. D., Takacs, L., Kim, G.-K., Bloom, S., Chen, J., Collins, D., Conaty, A., Arlindo da Silva, Gu, W., Joiner, J., Koster, R. D., Lucchesi, R., Molod, A., Owens, T., Pawson, S., Pegion, P., Redder, C. R., Reichle, R., Robertson, F. R., Ruddick, A. G., Sienkiewicz, M., and Woollen, J.: MERRA – NASA's modern-era retrospective analysis for research and applications, J. Climate, 24, 3624–3648, doi:10.1175/JCLI-D-11-00015.1, 2011.

AMTD
5, 5205–5243, 2012

Samet, J. M., Zegar, S. L., Dominici, F., Curriero, F., Coursac, I., Dockery, D. W., Schwartz, J., and Zanobetti, A.: The National Morbidity, Mortality, and Air Pollution Study Part II: Morbidity and Mortality from Air Pollution in the United States, Health Effects Institute, 94, 1–89, 2000.
Shi, Y., Zhang, J., Reid, J. S., Holben, B., Hyer, E. J., and Curtis, C.: An analysis of the collection 5 MODIS over-ocean aerosol optical depth product for its implication in aerosol assimilation, Atmos. Chem. Phys., 11, 557–565, doi:10.5194/acp-11-557-2011, 2011.
Smirnov, A., Holben, B. N., Giles, D. M., Slutsker, I., O'Neill, N. T., Eck, T. F., Macke, A., Croot, P., Courcoux, Y., Sakerin, S. M., Smyth, T. J., Zielinski, T., Zibordi, G., Goes, J. I., Harvey, M. J., Quinn, P. K., Nelson, N. B., Radionov, V. F., Duarte, C. M., Losno, R., Sciare, J., Voss, K. J., Kinne, S., Nalli, N. R., Joseph, E., Krishna Moorthy, K., Covert, D. S., Gulev, S. K., Milinevsky, G., Larouche, P., Belanger, S., Horne, E., Chin, M., Remer, L. A., Kahn, R. A., Reid, J. S., Schulz, M., Heald, C. L., Zhang, J., Lapina, K., Kleidman, R. G., Griesfeller, J., Gaitley, B. J., Tan, Q., and Diehl, T. L.: Maritime aerosol network as a component of AERONET – first results and comparison with global aerosol models and satellite retrievals, Atmos. Meas. Tech., 4, 583–597, doi:10.5194/amt-4-583-2011, 2011.
Taylor, K. E.: Summarizing multiple aspects of model performance in a single diagram, J. Geophys. Res., 106, 7183–7192, doi:10.1029/2000JD900719, 2001.
Tibbetts, J.: Coastal cities: living on the edge, Environ. Health Persp., 110, 674–681, 2002.
Wilks, D. S.: Frequentist Statistical Inference, in Statistical Methods in the Atmospheric Sciences, 3rd edn., Academic Press, San Diego, California, 2011.
Zhang, J. and Reid, J.: MODIS aerosol product analysis for data assimilation: assessment of over-ocean level 2 aerosol optical thickness retrievals, J. Geophys. Res., 111, 1–17, doi:10.1029/2005JD006898, 2006.
Zhang, J. and Reid, J. S.: A decadal regional and global trend analysis of the aerosol optical depth using a data-assimilation grade over-water MODIS and Level 2 MISR aerosol products, Atmos. Chem. Phys., 10, 10949–10963, doi:10.5194/acp-10-10949-2010, 2010.
Zhao, X.-P. T., Heidinger, A., and Knapp, K.: Long-term trends of zonally averaged aerosol optical thickness observed from operational satellite AVHRR instrument, Meteorol. Appl., 18, 440–445, doi:10.1002/met.235, 2011.

AMTD
5, 5205–5243, 2012

Table 1. MODIS AOD mean bias over the full data record (2002–2010) for all AERONET coastal stations. 62 coastal AERONET sites were identified and the results are an average of all the sites. Each of the MODIS aerosol algorithms is shown with the recommended quality control except for the Land_and_Ocean product which is shown without any quality control (default MODIS product) and the results of our quality control technique described in Sect. 4. Bias results are separated into Low AOD and High AOD events as classified by AERONET measurements with the cutoff at 0.25.

All Coastal Sites	Land Algorithm QA Filtered	Ocean Algorithm QA Filtered	Land_and_Ocean	
			No Filter	QA Filtered
Total Bias	0.026	0.006	0.029	0.019
Low AOD Bias	0.024	0.021	0.033	0.024
High AOD Bias	0.026	−0.029	0.026	0.010

AMTD
5, 5205–5243, 2012

Table 2. MODIS AOD bias with respect to AERONET AOD for both coastal and open ocean sites. The bias is listed for three categories on how MODIS AOD is used in the evaluation. The first is filtering of data with quality control flag; the second builds upon the first but also removes MODIS AOD data with cloud fraction larger than 80 %; the third is the same as second except the threshold for cloud fraction is now decreased to 70 %. The number of AOD retrievals used in the different analyses (last row in Table 2) is also shown to display the reduction in data size associated with each category. In each category, bias is further analyzed in terms of low AOD conditions (AOD < 0.25) and high AOD conditions. In addition, the relative percent change of bias due to the filtering of data with cloud fraction is shown in in parentheses, negative percentages indicate an increase in bias. See text for further details.

MODIS Cloud Contamination	Normal QA		80 % Threshold		70 % Threshold	
	Coastal	Open Ocean	Coastal	Open Ocean	Coastal	Open Ocean
Total Bias	0.006	0.012	0.002 (67 %)	0.008 (33 %)	0.000 (100 %)	0.005 (58 %)
Low AOD Bias	0.021	0.018	0.018 (14 %)	0.013 (28 %)	0.016 (24 %)	0.011 (39 %)
High AOD Bias	−0.029	−0.022	−0.035 (−21 %)	−0.026 (−18 %)	−0.035 (−21 %)	−0.027 (−23 %)
Number of Retrievals	18 001	4190	17 104	3441	15 768	3118

AMTD
5, 5205–5243, 2012

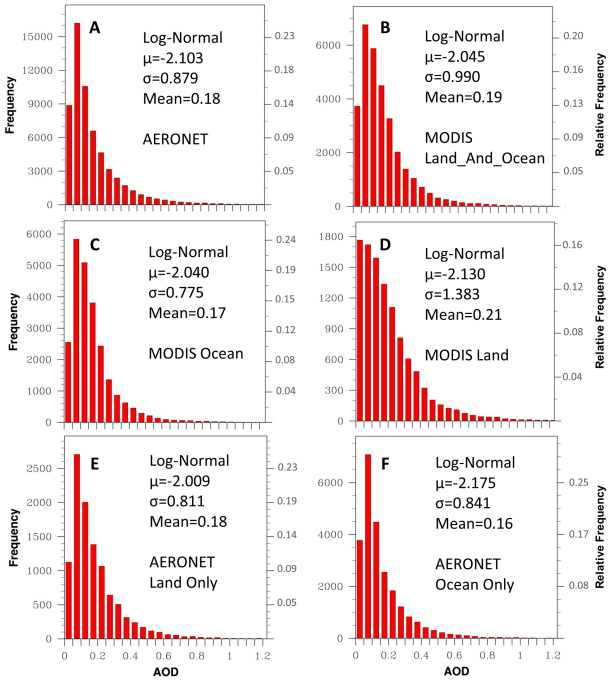

Fig. 1. Frequency of coastal AOD (left vertical axis) and relative frequency of AOD (right vertical axis) at AERONET sites over the ∼9 yr period from ∼2002–2010. Plots are derived from AOD data at 62 coastal AERONET sites and collocated MODIS retrievals over those sites. μ is the log-normal location parameter and σ is the log-normal scale parameter, mean is the average AOD over the whole time period. **(A–E)** respectively show quality assured and quality flag filtered frequency of AOD from AERONET, Land algorithm, Ocean algorithm, MODIS Land_and_Ocean product, and from AERONET AODs paired with MODIS AOD from Land algorithm only, and AERONET AODs paired with MODIS AOD from Ocean algorithm only.

AMTD
5, 5205–5243, 2012

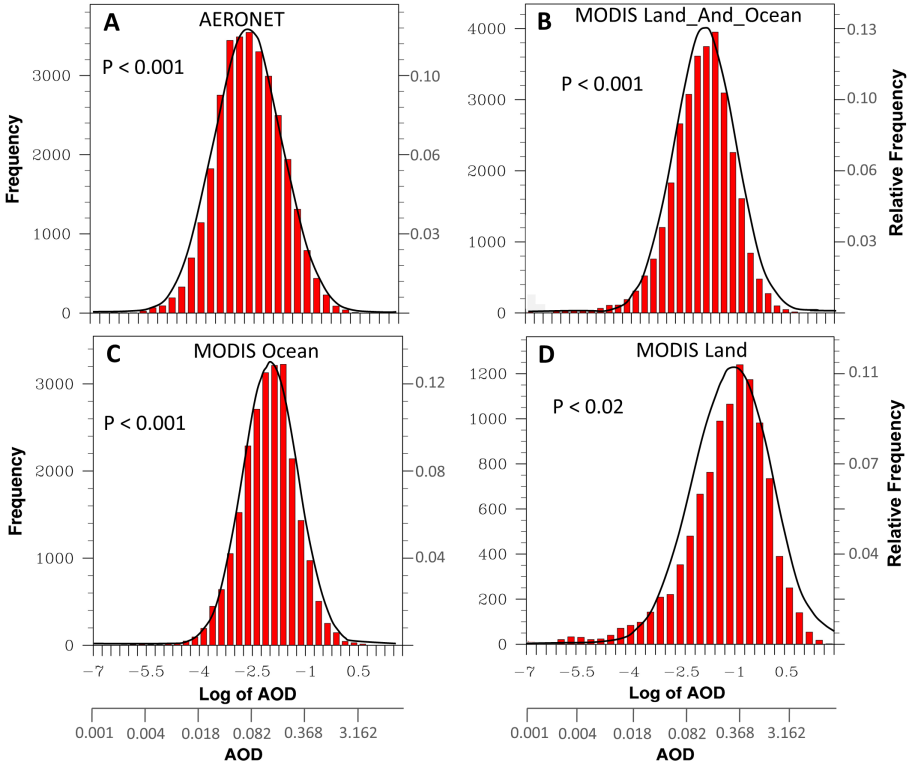

Fig. 2. PDFs (right vertical axis) and frequency (left vertical axis) of the coastal AODs from **(A)** AERONET, **(B)** MODIS Land_and_Ocean, **(C)** MODIS Ocean algorithm, and **(D)** MODIS Land algorithm. All MODIS algorithms are quality flag filtered and the data span from ~2002–2010. The p-values indicate statistical significance of fitness between frequency distributions derived from PDFs (e.g. product of total number of data points, PDFs, and AOD bin interval) and actual frequency distribution (e.g. the bars in red). See text for details. **(A)** Has only those AOD observations when there was a corresponding MODIS AOD retrieval.

AMTD
5, 5205–5243, 2012

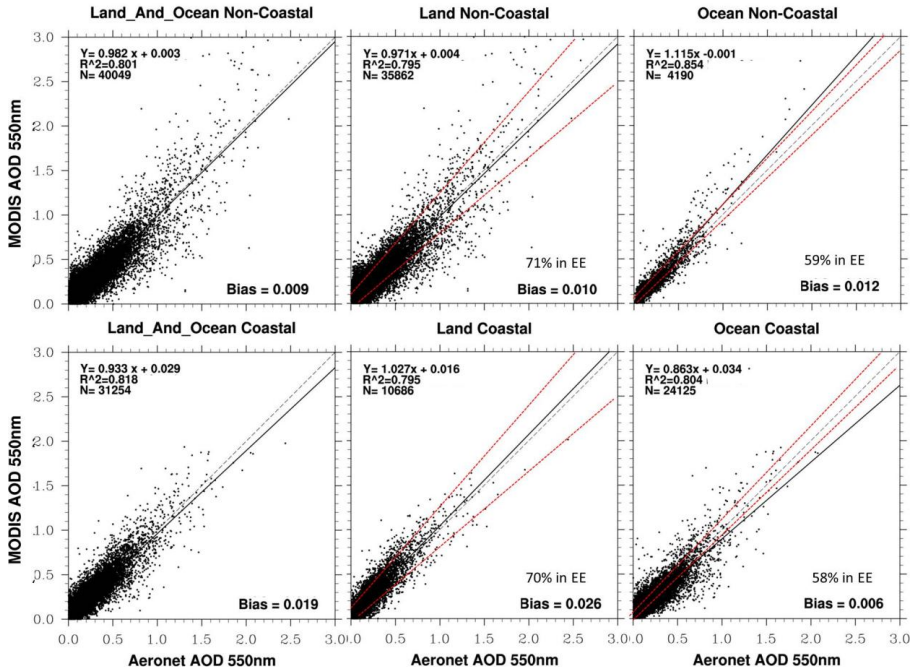

Fig. 3. Scatter plot of AERONET AOD (x-axis) and the quality flag filtered MODIS AOD (y-axis) from ~2002–2010. In (**A**, **B**, and **C**), AODs in y-axis are respectively derived from MODIS Land_and_Ocean, Land, and Ocean products over the non-coastal AERONET stations (**D**, **E** and **F**) are respectively the same as (**A**, **B**, and **C**) but over the coastal AEROENT stations. In each scatter plot, also shown is the correlation coefficient (R^2), mean bias, the number of MODIS-AERONET collocated data points (N), and the best-fit linear regression equation (solid black line), the 1 : 1 line (dashed black line), and the expected error envelope (red dashed line) for MODIS AOD explained in Sect. 3.2.

AMTD
5, 5205–5243, 2012

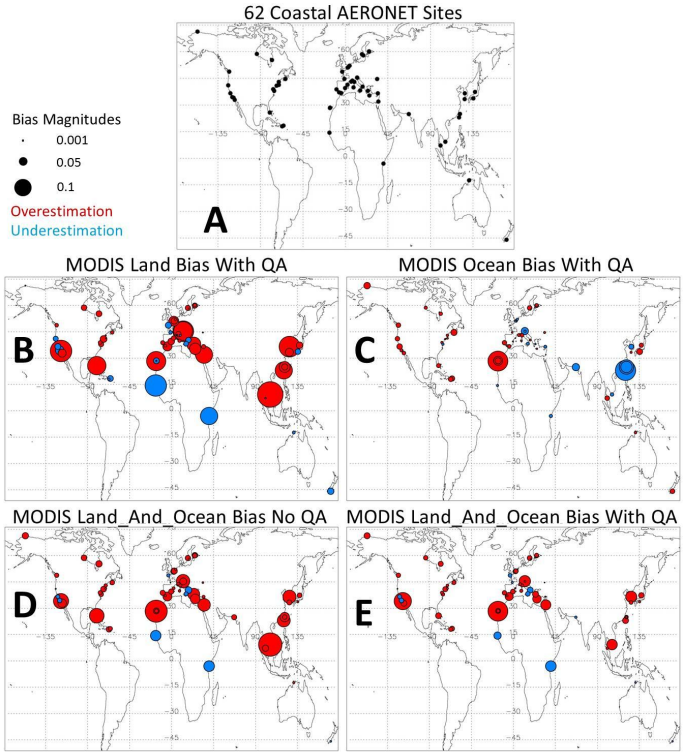

Fig. 4. (A) Map of the location of all coastal AERONET sites; **(B–E)** show the maps of MODIS AOD bias (with respect to AERONET AOD) at each coastal AERONET site respectively for: **(B)** MODIS Land AOD product filtered with quality flag, **(C)** MODIS Ocean AOD product filtered with quality flag; **(D)** MODIS Land_and_Ocean AOD product without any quality filtering; **(E)** MODIS Land_and_Ocean aerosol product after using the method described in the Sect. 4 for quality filtering. Bias calculations are based on ∼9 yr (2002–2010) of collocated MODIS and AERONET AOD data. Blue indicates MODIS underestimation of AOD (e.g. negative bias) and red is overestimation (positive bias). Common legend is left of panel **(A)**.

AMTD
5, 5205–5243, 2012

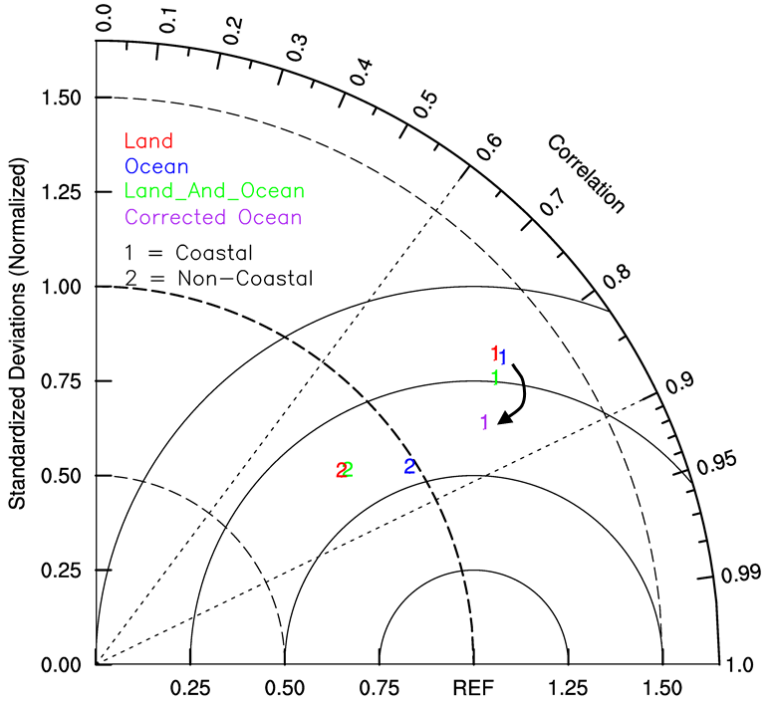

Fig. 5. Taylor diagram comparing ~2002–2010 quality flag filtered MODIS AOD retrievals and AERONET AOD observations. Coastal MODIS AOD retrievals are listed with a 1 and Non-Coastal AODs are shown with a 2. The MODIS Ocean, Land, Land_and_Ocean, and empirically corrected Ocean (see Sect. 5) products are represented by blue, red, green, and purple respectively The arrow represents the effect of the empirical correction on the MODIS Ocean product.

AMTD
5, 5205–5243, 2012

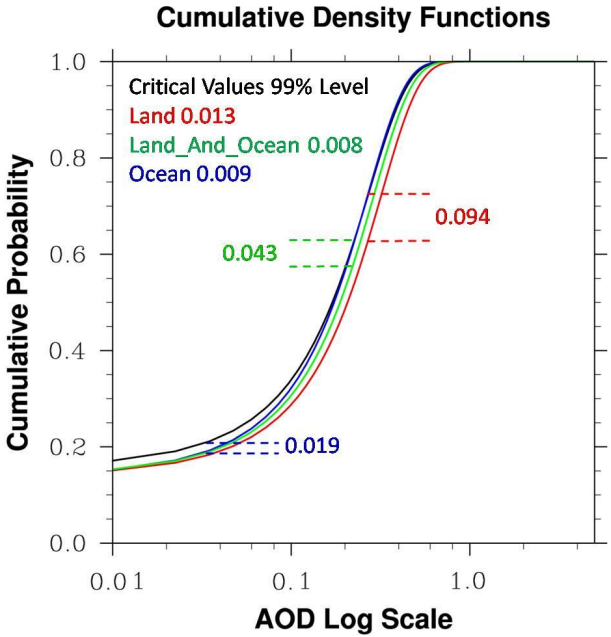

Fig. 6. Cumulative density functions (CDF) of AOD derived from AERONET (black), and corresponding paired MODIS AODs respective derived from MODIS Land (red), Ocean (blue), and Land_and_Ocean (green) products after filtering with quality flag. These CDFs are based upon the log-normal distributions with parameters shown in Fig. 2. Maximum differences between the AERONET CDF and MODIS CDFs are shown by two dashed lines in their respective colors. Data are from MODIS from ~ 2002–2010 over coastal regions. Critical value and K-S test are described in text (Sects. 3.1 and 3.2). When the difference is greater than the critical values there is a statistically significant difference between the MODIS and AEROENT CDFs.

AMTD
5, 5205–5243, 2012

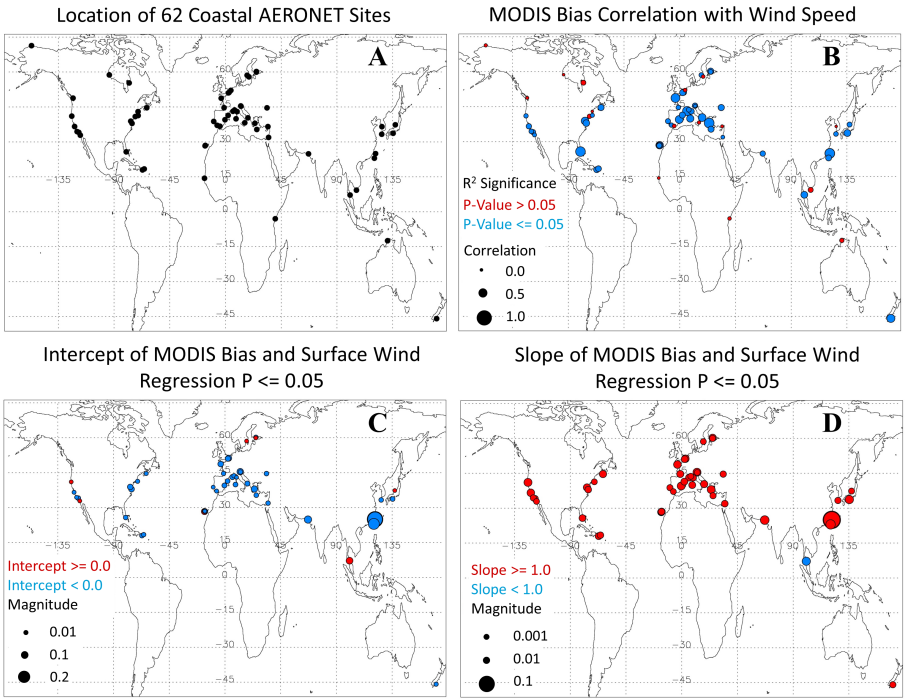

Fig. 7. (A) Station locations for each coastal AERONET site **(B)** the correlation between quality flag filtered MODIS Ocean algorithm AOD bias and sea-surface wind speed **(C)** the *y*-intercept from the linear regression of bias and wind speed **(D)** the slope from the linear regression of bias and wind speed. Blue colors represent statistically significant values in **(B)** and negative intercepts and slopes for **(C)** and **(D)**, respectively. Red represents statistically insignificant values in **(B)** and positive intercepts and slopes for **(C)** and **(D)**, respectively. Magnitude scales are provided in each panel for clarity. **(C)** and **(D)** show only sites with p-value less than or equal to 0.05 (46 out of the possible 62 sites). Data are from ~2002–2010.

AMTD
5, 5205–5243, 2012

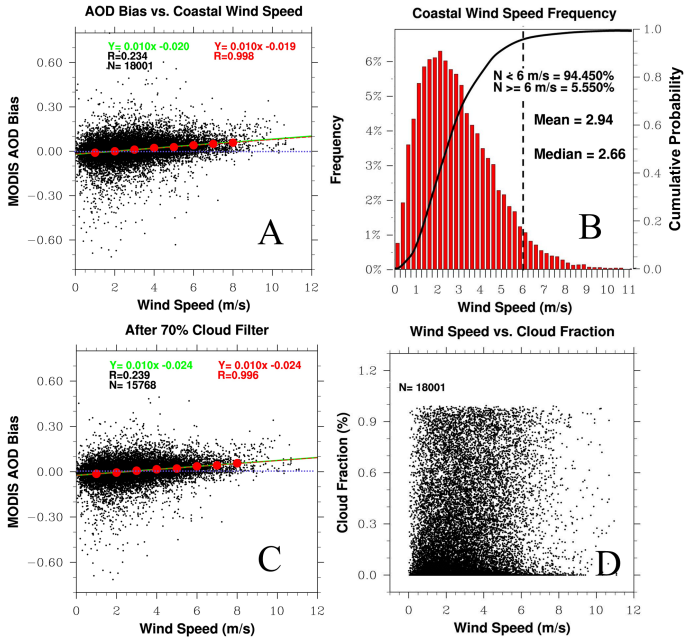

Fig. 8. (A) Scatter plot of quality flag filtered MODIS Ocean AOD bias against the 2 m wind speed from MERRA, **(B)** the frequency of coastal wind speeds during MODIS overpass times, **(C)** same as **(A)** but for the bias of MODIS AOD after 70 % cloud fraction filter, **(D)** scatter plot of the wind speed and cloud fraction pairs for each retrieval. The analysis is for all coastal sites (62 AERONET sites) and for the years ∼ 2002–2010. *R* is the Pearson linear correlation coefficient, *N* is the number of retrievals and *Y* is the regression equation. In **(B)**, the right vertical axis is the cumulative density function for the coastal wind speeds (represented by the black curve). In **(A)** and **(C)** red is MODIS bias binned to 1 $m s^{-1}$ intervals along with regression and correlation corresponding to those bins, and the blue dotted line is a reference 0 MODIS bias.

AMTD
5, 5205–5243, 2012

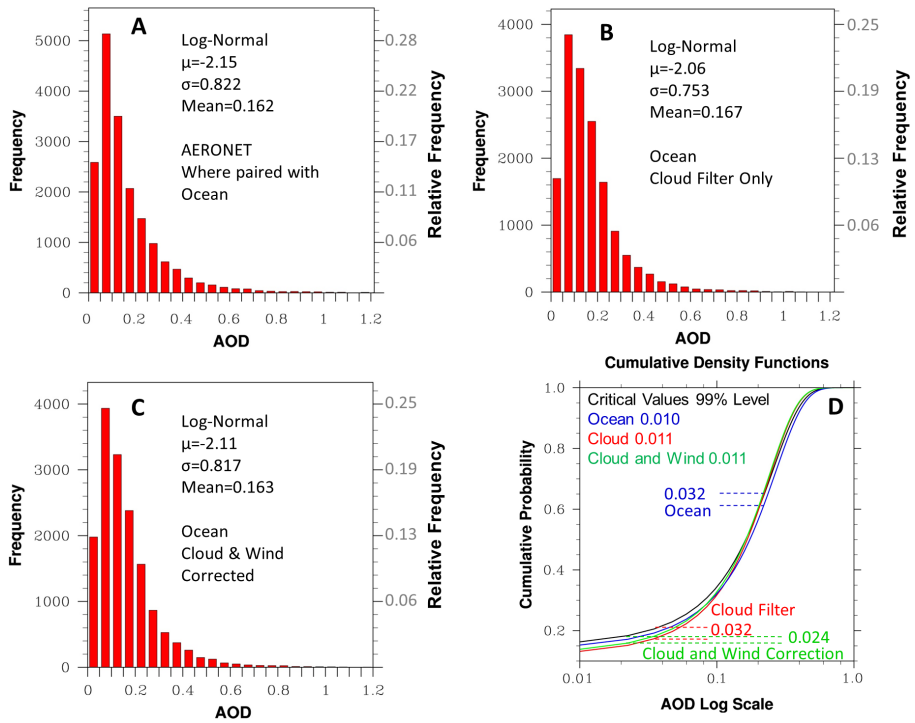

Fig. 9. Frequency distribution of quality assured **(A)** AERONET AOD over coastal regions that have an MODIS Ocean algorithm collocated retrieval, **(B)** AOD from MODIS Ocean algorithm after cloud fraction and quality flag filtering only **(C)** AOD from MODIS Ocean algorithm after cloud fraction filtering (70 %), wind speed bias correction, and quality flag filtering, **(D)** cumulative density functions (CDF) derived from the frequency distributions respectively in **(A)**–**(C)**, along with their respective maximum difference from the AERONET CDF. Quality flag filtering is applied for all algorithms and the MODIS data span ~2002–2010. The critical values and K-S test from panel **(D)** are described in Sects. 3.1 and 5 in the text.

AMTD
5, 5205–5243, 2012